JOURNAL OF OPTOELECTRONICS AND ADVANCED MATERIALS Vol. 9, No. 8, August 2007, p. 2327 - 2338

Characterization of laser beam parameters for optical microfabrication of ultrahard and wide band gap photonic materials for MOEMS applications

S. K. SUDHEER*, N. VENUGOPALAN PILLAI[a], V. P. MAHADEVAN PILLAI[a], ZACHARIAH C. ALEX, V. U. NAYAR[a]
School of Electrical Sciences,Vellore Institute of Technology , Katpadi, Vellore- 632014, Tamilnadu, India
[a]Department of Optoelectronics, University of Kerala, Kariavattom, Thiruvananthapuram-695 581, Kerala, India

The laser beam parameters of a lamp pumped Q-switched Nd:YAG laser have been characterized for ultra hard wide band gap photonic material.

(Received February 19, 2007; accepted July 10, 2007)

Keywords: Photonic materials, Nd:YAG laser, MOEMS

1. Introduction

MOEMS (Micro-Opto-Electro-Mechanical Systems) are devices that couples photons with electronics and micro machined structures or mechanical motion in some way on the micron scale. Some devices such as the monolithically integrated optical displacement measurement Microsystems contains some form of active lens or mirror, and will ultimately meet the criteria of true optical MEMS. Lasers are employed in pattern generation and replication, for removing and depositing materials in patterns for metrology of MEMS. Temporal characteristics of these lasers ranges from femtosecond pulse widths to continuous wave operation. An evaluation of lasers and optical systems for MOEMS production ultimately depends on three main characteristics of a MOEMS design and are optical properties of the material,thermal properties of the material and geometric form of the part.The evaluation of these factors dictates the required characteristics of the laser.Various laser beam parameters like beam diameter, divergence, ellipticity, beam waist size, beam focusability factor (M^2 parameter) and laser crystal sensitivity factor are the important parameters which are to be addressed while designing a laser system for material processing application. Generation of laser beam in the high power TEM_{00} mode is a mandatory condition for ultrahard wide band gap photonic material like natural diamond processing [1]. Very good beam quality provides very small beam focusability factor which produces extremely small focused spot and consequently high energy density at the work piece. Laser beam focusability factor also known as M^2 parameter, plays an important role in laser micro fabrication [2]. This quantifiable factor is a measure of how close the laser beam is to a perfect Gaussian beam. A perfect TEM_{00} Gaussian beam has an M^2 factor equal to unity; where as an imperfect beam will have a value greater than unity.

Various aspects of laser beam parameters for processing ultrahard materials have been reported previously [3-5]. The thermal dependence of active medium and other beam parameters have been reported [6,7]. As the input pump power is applied to the laser crystal, thermal stress is induced inside it which produces mechanical deformations at its free end faces. As a result the laser rod acts as a thick lens which is referred to as thermal lens and it focuses the laser beam generated by it. The dioptric power of the thermal lens formed is proportional to the input pump power and it determines many of the mode characteristics of the laser beam. In a laser system with planar resonator configuration, the cross section of the mode inside the rod is large and hence any changes in the dioptric power of thermal lens may have a strong effect upon the diffraction losses of the mode [8].

In the present investigation, the laser beam parameters of a lamp pumped Q-Switched Nd:YAG laser have been characterized for ultra hard wide band gap photonic material processing application.

2. Experimental

The experimental setup for the measurement of laser beam parameters is given in Fig. 1.

Photon Inc(USA) Model 0180 Beam Scan beam profiler system with Model XYQSW Scan head connected to computer with 0810 Plug-In controller card is used for the beam parameter measurements. The main components of the scan head are the rotating drum with an air slit and a stationary large area detector nested between the drum and the motor to collect light transmitted by the air slit. The scan head is aligned in the beam path to be measured so that the slit passes through the beam and exposes the detector. The transmitted photons cause current to flow from the detector to load resistor. The voltage across the resistor is proportional to the beam irradiance profile. The

irradiance profile is measured as the slit scans through the beam.

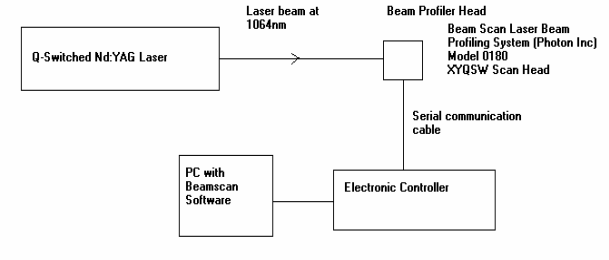

Fig. 1. Experimental setup of laser beam profiler to measure the various laser beam parameters.

The beam profiler uses slit- width clip level beam size method, where a photo detector collects the intensity profile of the beam seen by a very narrow moving slit. The peak voltage observed is arbitrarily set to 100% and tail extremes are set to 0%. As per the definitions of ISO standards, the beam diameter is measured as the spatial width at an irradiance clip level of 13.5% (). In the slit width clip level beam size method [9], the irradiance profile seen at a very narrow slit is collected.

The effect of Nd^{3+} doping concentration on the beam parameters is studied for three Nd concentrations (0.8 at. %, 0.7 at.% and 0.65 at.%) of the Nd:YAG rods (3ϕ x 108mm dimensions). The measurements are carried out in both CW and Q-Switched operation. It is the TEM_{00} mode which is used in the present studies.

3. Results and discussion

3.1 CW Operation

The variation of beam diameter and ellipticity with input electrical power is plotted for the three Nd doping concentrations in Figs. 2 and 4 respectively.

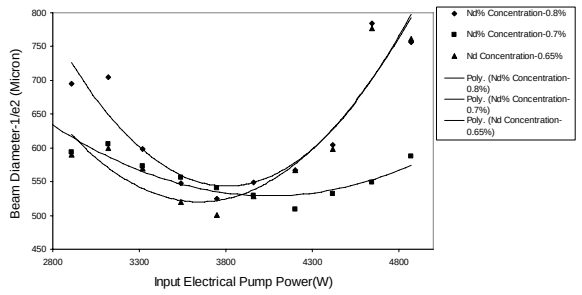

Fig. 2. Variation of Beam diameter of laser beam with input power at various Nd concentrations of active medium.

Second order polynomials are fitted with the data where the standard error is minimum and the coefficients of the polynomials are shown in Table 2 below.

Table 2. Coefficients of second order polynomial fitted with the data.

No	Nd doping concentration (%)	Coefficients of second order polynomial term		
		X^2	X	Constant Term
1	0.8	0.000225	-1.713618	3806.508284
2	0.7	0.0000666	-0.5401794	1623.786717
3	0.65	0.000182	-1.328172	2942.667956

It is observed that the beam diameter is minimum for a particular pump power P_{in}* and its value varies with different Nd doping concentration. The input power P_{in}* for which the beam diameter is minimum is calculated for different doping concentrations from the curves shown in Fig. 3.2 and are given in the Table 3. Also minimum beam diameters for the three concentrations are calculated from Fig. 3.

Table 3.3. Variation of P_{in} and w* for different Nd doping concentrations.*

No	Parameter	Nd doping concentration (%)		
		0.8	0.7	0.65
1.	P_{in}*	3808.04	4055.401	3648.824
2	w*	543.7453	528.4647	519.5349

The input power P_{in}* for the three Nd doping concentrations are in the order

$$P_{in-0.7}^{*} > P_{in-0.8}^{*} > P_{in-0.65}^{*} \quad (1)$$

The minimum beam diameter w* for these concentrations are in the order

$$w^*_{0.65} < w^*_{0.7} < w^*_{0.8} \quad (2)$$

The variation of the minimum beam diameter with Nd doping concentrations is plotted in Fig. 3.

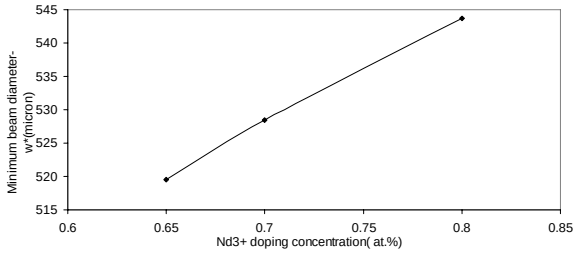

Fig. 3. Variation of the minimum beam diameter with Nd doping concentrations.

The variation of laser beam size at the output coupler with input electrical pump power can be interpreted using matrix representation of the passive and active resonators. The matrix representation for the passive laser resonator without the laser crystal, using ABCD law is

$$\begin{pmatrix} 1 & 0 \\ \frac{-1}{R_2} & 1 \end{pmatrix}\begin{pmatrix} 1 & L \\ 0 & 1 \end{pmatrix}\begin{pmatrix} 1 & 0 \\ \frac{-1}{R_1} & 1 \end{pmatrix}=\begin{pmatrix} 1-\frac{L}{R_1} & L \\ \frac{-1}{R_1}-\frac{1}{R_2}+\frac{L}{R_1R_2} & 1-\frac{L}{R_2} \end{pmatrix}=\begin{pmatrix} g_1 & L \\ \frac{g_1g_2-1}{L} & g_2 \end{pmatrix} \tag{3}$$

Where g_1 and g_2 are the stability parameters given by $g_1=1-\frac{L}{R_1}$, $g_2=1-\frac{L}{R_2}$, $R_1$and R_2 are the radii of curvatures of the two mirrors and L-the resonator length.

Since the active material possesses a saturable non-uniform gain and exhibits thermal lensing and thermally induced birefringence, the introduction of an active element into the resonator results in the altering of the optical length of the resonator, and perturbation of the mode configuration. Optical pumping leads to a radial temperature gradient in the laser rod. As a result, the rod acts like a thick lens of an effective focal length f_e which is inversely proportional to the pump power P_{in}. In the present investigation, as the resonator configuration is plane parallel, $R_1=R_2=\infty$. Thus on introduction of laser crystal between the end mirrors, the ABCD matrix changes to

$$\begin{pmatrix} 1 & 0 \\ 0 & 1 \end{pmatrix}\begin{pmatrix} 1 & L_2 \\ 0 & 1 \end{pmatrix}\begin{pmatrix} 1 & 0 \\ \frac{-1}{f_e} & 1 \end{pmatrix}\begin{pmatrix} 1 & L_1 \\ 0 & 1 \end{pmatrix}\begin{pmatrix} 1 & 0 \\ 0 & 1 \end{pmatrix}=\begin{pmatrix} 1-\frac{L_2}{f_e} & L_1+L_2-\frac{L_1L_2}{f_e} \\ \frac{-1}{f_e} & 1-\frac{L_1}{f_e} \end{pmatrix}=\begin{pmatrix} g_1^* & L_{eff} \\ \frac{-1}{f_e} & g_2^* \end{pmatrix} \tag{4}$$

where g_1^* and g_2^* are the modified stability parameters, L_1 and L_2 are the distances from the two end mirrors and centre of laser crystal and L_{eff} is the effective resonator length and are given by

$$g_1^*=1-\frac{L_2}{f_e} \tag{5}$$

$$g_{*2}^*=1-\frac{L_1}{f_e} \tag{6}$$

$$L_{eff}=L_1+L_2-\frac{L_1L_2}{f_e} \tag{7}$$

Since the thermal lens focal length f_e is inversely proportional to input pump power P_{in},

$$f_e=\frac{1}{\alpha P_{in}} \tag{8}$$

$$L_{eff}=L_1+L_2-L_1L_2\alpha P_{in} \tag{9}$$

For a planar resonator, the TEM_{00} mode spot at one of the mirrors can be expressed as a function of the resonator parameters as

$$w_1^2=\frac{\lambda L_{eff}}{\pi}\left(\frac{g_2^*}{g_1^*(1-g_1^*g_2^*)}\right)^{1/2}$$

$$w_1^2=\frac{\lambda(L_1+L_2-L_1L_2\alpha P_{in})}{\pi}\left(\frac{g_2^*}{g_1^*(1-g_1^*g_2^*)}\right)^{1/2} \tag{10}$$

In the present investigation where two plane mirrors are used as end mirrors so that $R_1 = R_2 = \infty$ and it is assumed that a thin lens in the center $(L_1 = L_2 = \frac{L}{2})$.

From equations (5) and (6) it is obtained that

$$g^*=g_1^*=g_2^*=1-\frac{L}{2f_e} \tag{11}$$

$$w_1^2=w_2^2=\left(\frac{\lambda L_{eff}}{\pi}\right)\left(1-g^{*2}\right)^{-1/2} \tag{12}$$

Case 1: With no thermal lens, the resonator is plane parallel (with $P_{in} = 0$), , $f_e = \infty$ and w_1 tends to infinity as obtained in Fig. 2 for the three Nd^{3+} doping concentrations.

Case 2: As Pin increases w_1 decreases and reaches a minimum value w* when the resonator configuration is equivalent to a confocal one and $f_e=\frac{L}{2}$. then

$$w_1^2=\left(\frac{\lambda L_{eff}}{\pi}\right)_{Pin=Pin^*} \tag{13}$$

The value of w* is found increasing with increase in Nd^{3+} doping concentration as shown in Fig. 3.

Case 3: As Pin increases beyond this value, thermal lens focal length decreases and when $f_e=\frac{L}{4}$, the resonator goes to a spherical configuration. The mode size w_1 in the resonator will grow to infinity as the mirror

separation approaches four times the focal length of the rod which is evidenced from Fig. 2 for the three Nd^{3+} concentrations.

The ellipticity of the laser beam is measured at different pump power for the three different Nd doping concentrations. The variations are shown in shown in Fig. 4.

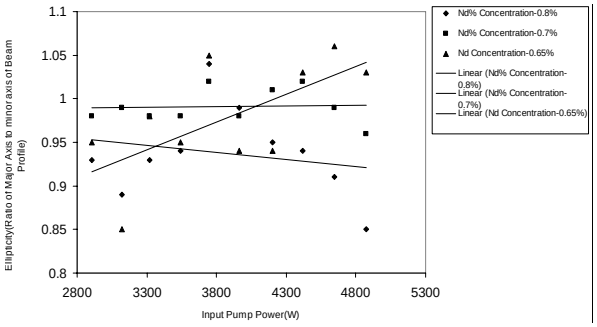

Fig. 4. Variation of ellipticity of laser beam with input power at various Nd concentrations of active medium.

Linear fitting is performed with the data where the standard error is minimum and coefficients of various terms of fitted line are shown in Table 3 below.

Table 3. Coefficients of terms of line fitted with the data.

No	Nd doping concentration (%)	Coefficients of terms of line fitted with the data	
		X	Constant Term
1	0.8	-0.000016	1.000864
2	0.7	0.000002	0.984208
3	0.65	0.000064	0.731659

Ellipticity of a laser beam is the ratio of vertical beam diameter to that in the horizontal direction. For an ideal laser beam with perfect pumping geometry, the ellipticity will be unity which means that the beam is perfectly circular. From Fig. 4, it can be seen that the ellipticity of the beam for 0.7 at.% Nd concentration remains almost unity throughout the complete range of input power. In Table 1, it is seen that for the Nd doping concentration of 0.8 at.%, the value of ellipticity first increases from a value of 0.93 to a value near to unity at around P_{in}* (3808.04 W) and then decreases with increase of P_{in} to a value lower than unity. For $P_{in}>P_{in}$* and $P_{in}<P_{in}$* the cross section of the beam is horizontal ellipse where as it approaches circular symmetry at around P_{in}*. For Nd doping concentration of 0.65 at.%, as the input pump power increases, the value of ellipticity also increases from a value less than unity (Fig. 3.4). Hence the cross section of the beam is horizontal ellipse when $P_{in}<P_{in}$*,circular around P_{in}* (3648.82 W) and vertical ellipse when $P_{in}>P_{in}$*. As the 0.7 at.% doped laser crystal exhibits comparatively broad operating range of input pump power over which the output laser beam possess good circular symmetry, it is preferred to others for efficient processing of diamond crystals.

3.2 Q-Switched operation

Nd: YAG crystal ($3\phi \times 108$ mm) with 0.7 at.% doped has been used for the laser operation in Q-Switched mode since ellipticity of the beam remains good over the complete range of input power. The laser is operated in the Q-Switched mode at a frequency of 8 KHz. The frequency selection is done based on the following facts. At higher Q-Switched frequencies above 12 KHz, the peak power may not be sufficient for material removal. At lower frequencies below 4 KHz, the peak power is too high and it may produce micro cracking inside the diamond crystal which is undesirable. In order to ensure the safety of the delicate Scan Head of beam profiler used for the measurements, an expanded beam with expansion ration 8 is used in the investigations in Q-Switched mode.

The beam diameter in both vertical and horizontal directions, ellipticity and divergence in both vertical and horizontal directions are measured at different values of average laser output power. The variation of the beam diameter $\left(\frac{1}{e^2}\right)$ with average power is plotted and shown in Fig. 5 below.

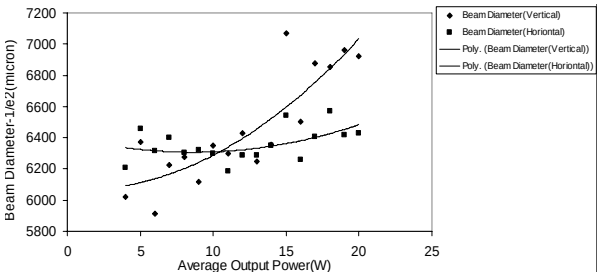

Fig. 5. Variation of beam diameter of laser beam (expanded 8 times) in vertical and horizontal directions with average power of the Q-switched laser at 8 KHz repetition rate.

Second order polynomials are fitted with the data for which standard error is obtained as minimum and coefficients are shown in Table 7.

Table 7. Coefficients of terms of second order polynomial of beam diameter data.

No	Direction	Coefficients of terms of second order polynomial			Standard Error of the least square fit
		X^2	X	Constant Term	
1	Vertical	2.6271	-4.1598	6067.2	713.6897
2	Horizontal	1.3687	-23.628	6408.9	367.7907

Beam diameter $\left(\frac{1}{e^2}\right)$ in horizontal direction is found to be increasing slightly with increase in Pin where as that in vertical direction shows a larger increase. This is an indication that the thermo-optic coefficient values of crystal along these directions are different resulting in different thermal lens focal lengths and beam propagation factors in the respective directions [9-11].

The ellipticity of the beam in the Q-switched mode is measured at a Q-switched frequency of 8 KHz at different output average power of laser. The variation is shown in Fig. 6.

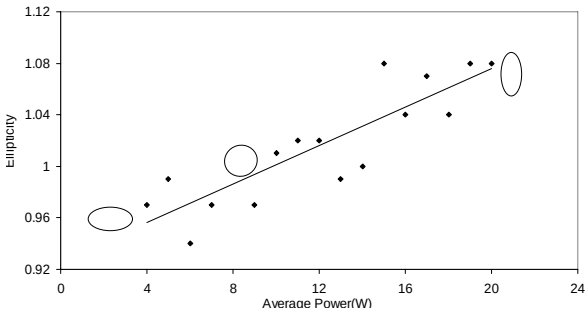

Fig. 6. Variation of ellipticity of output laser beam of Q-Switched Nd:YAG laser at various output average power.

It is observed that in CW mode of operation with 0.7 at.% Nd concentration the ellipticity remains almost close to unity throughout the input power range. However in the Q-switched operation this is not seen .When the output power is in the range 8-12 Watt, the ellipticity is almost near to unity. Below 8 W, it is found to be less than unity which indicates that the beam is horizontal ellipse. At output power levels greater than 12 W, the ellipticity is much above unity which is showing that the beam cross section is vertical ellipse. This may be due to thermally induced birefringence inside the laser crystal [12, 19, 20]. It is reported that the principal axes of the induced birefringence are radially and tangentially directed at each point in the rod cross section and that the magnitude of the birefringence increases quadratically with radius r [13,14]. As a consequence a linearly polarized TEM_{00} beam passing through the laser rod will experience a substantial depolarization. For a system with intra cavity Brewster window, the effect of depolarization involves the coupling of power into the orthogonal state of polarization followed by subsequent removal of that component by the polarizer and modification of the main beam by the depolarization process leading to a distortion of beam shape [15-18]. The variation from horizontal to vertical ellipse with change in average power agrees with the above facts. This measurement is very much helpful to decide a suitable power range within which we can operate the laser can be operated to get nearly perfect circularly symmetric beam for processing of diamonds.

The full angle divergence of the beam in both vertical and horizontal directions in Q-switched operation is measured at different output average power and the variation is plotted as shown in Fig. 7.

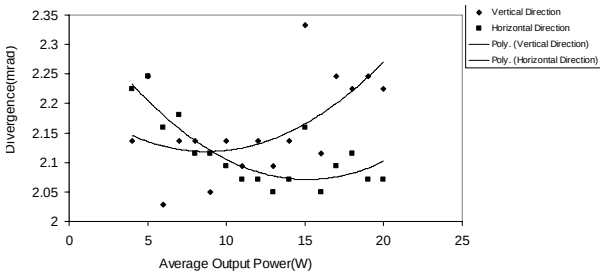

Fig. 7. Variation of divergence of output laser beam of Q-Switched Nd: YAG laser at various output average power.

Second order polynomials are fitted with the data for which minimum standard error is obtained and the coefficients are shown in Table 8.

Table 8. Coefficients of terms of polynomial of beam divergence data.

No	Direction	Coefficients of terms of polynomial		
		X^2	X	Constant Term
1	Vertical	0.001204	-0.021091	2.210867
2	Horizontal	0.0013	-0.0394	2.3695

With increase in average output power of the laser, the full angle divergence decreases first, reaches a minimum value and then increases in both horizontal and vertical directions. It is observed that the ellipticity approaches unity in the range of average power 8-12 W. In the case of full angle divergence in both directions, it remain almost

the same in this range. It can be assumed that the thermo-optic behavior of the laser crystal in this range is uniform in both directions. In the present study to collimate the beam and to reduce the divergence, a beam expander with expansion ratio 8 (Linos AG, Germany) was used before focusing.

3.3 Studies on the changes in Laser Beam Profiles

It is possible to study the Gaussian nature, circular symmetry (2D) and intensity distribution in space (3D) of the laser beam using beam profiler at different values of input pump lamp current. Such measurements are useful for determining the exact operating range of the laser for which one can obtain good results. The Gaussian, three dimensional and two dimensional and Gaussian intensity profiles of the CW laser beam were measured using laser beam profiler at arc lamp currents of 19 A, 25 A and 30 A and are shown in Figs. 8, 9 and 10, respectively.

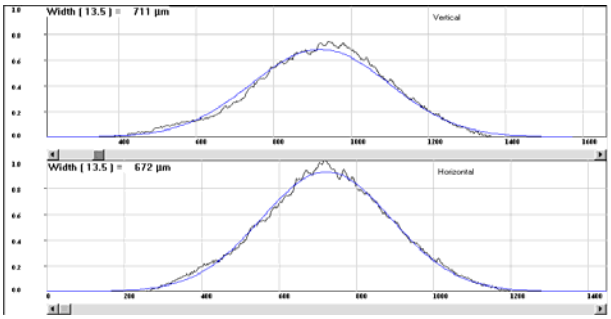

Fig. 8.1. Gaussian intensity profiles in vertical and horizontal directions of the beam at I_L=19 A (blue lines indicate the theoretical Gaussian fit).

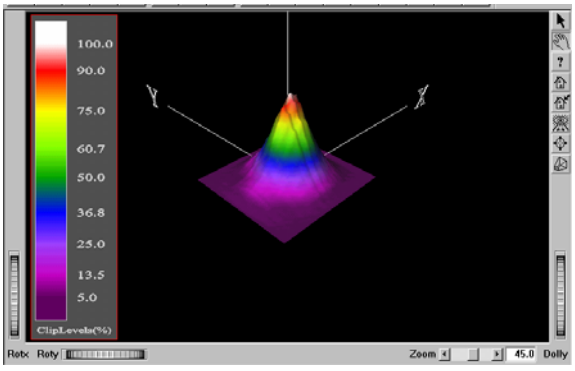

Fig. 8.2. Three dimensional intensity profile of beam at I_L= 19 A.

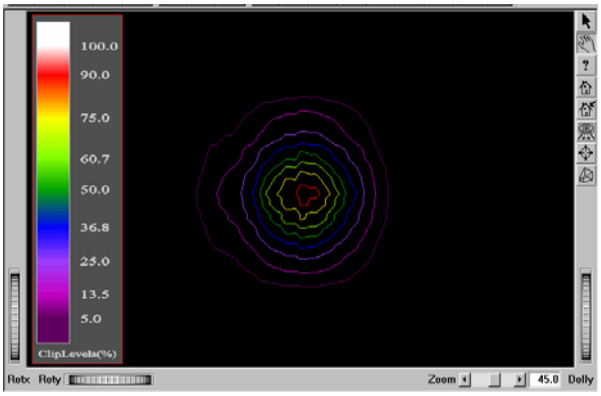

Fig. 8.3. Two dimensional intensity profile of beam at I_L= 19 A.

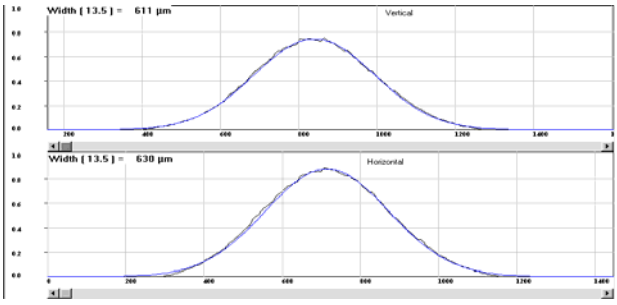

Fig. 9.1. Gaussian intensity profiles in vertical and horizontal directions of the beam at I_L=25 A (blue lines indicate the theoretical Gaussian fit).

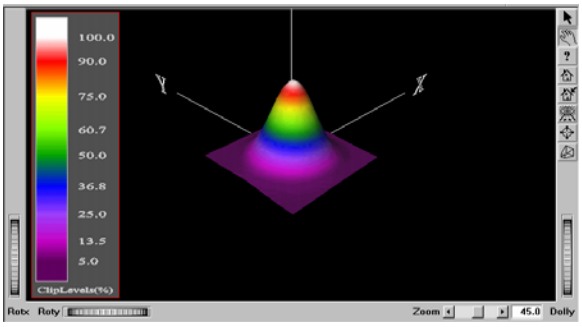

Fig. 9.2. Three dimensional intensity profile of beam at I_L= 25 A.

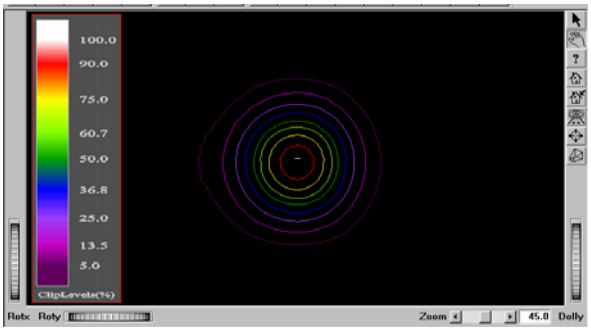

Fig. 9.3. Gaussian intensity profiles in vertical and horizontal directions of the beam at I_L=30 A (blue lines indicate the theoretical Gaussian fit).

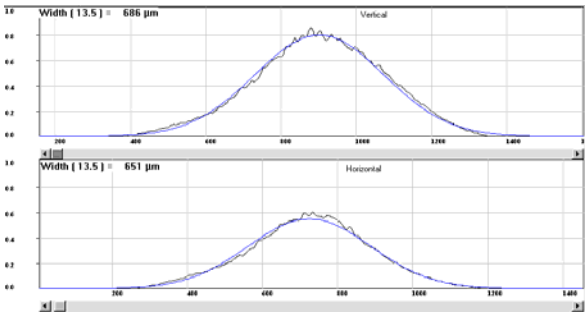

Fig. 10.1. Gaussian intensity profiles in vertical and horizontal directions of the beam at an arc lamp current of 30 A (blue lines indicates the theoretical Gaussian fit).

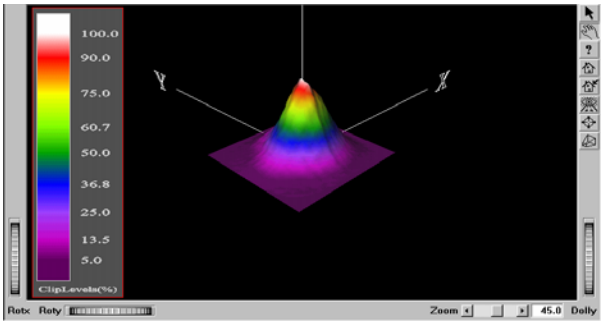

Fig. 10.2. Three dimensional intensity profile of beam at I_L= 30 A.

From the laser beam profiles it is observed that at lower pump powers for which $P_{in} < P_{in}$* and for higher pump powers $P_{in} > P_{in}$*, the beam profile is highly distorted and the deviation from Gaussian intensity distribution is more. At lower pump powers, as the pump energy is not sufficient for uniform pumping of rod and hence not concentrated towards to axial region of laser rod. As a result, the beam profile is not at all matched with Gaussian and it exhibits no circular symmetry. From Table 3, it is known that P_{in}* for 0.7% Nd doped YAG crystal is 4055.401 W and the P_{in} corresponds to an arc lamp current of 25A is 4200 W. Thus as the pump power increases to a value almost equal to P_{in}* the beam profile improves in quality and shows excellent Gaussian profile and circular symmetry. At higher pump powers higher than P_{in}*,the thermal stresses, thermal lensing and thermally induced birefringence of the laser crystal induce distortions inside the laser crystal and as a result output power decreases and beam profile deviates from Gaussian nature.

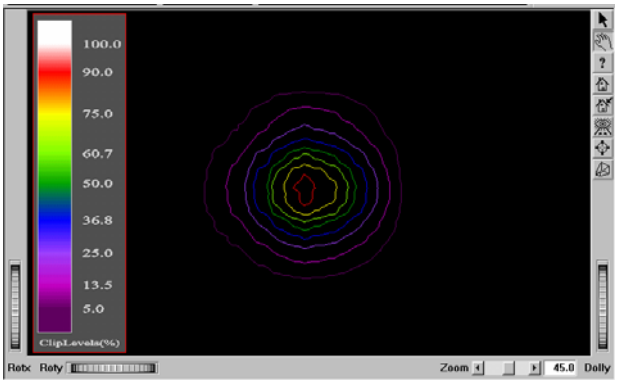

Fig. 10.3. Two Dimensional intensity profile of beam at a lamp current of 30A.

To get a clearer understanding of the variation of beam profile with pump power, profiles are recorded at different arc lamp currents continuously from 19A to 30A. The Gaussian, three dimensional and two dimensional and Gaussian intensity profiles recorded are shown in Figs. 11, 12 and 13, respectively.

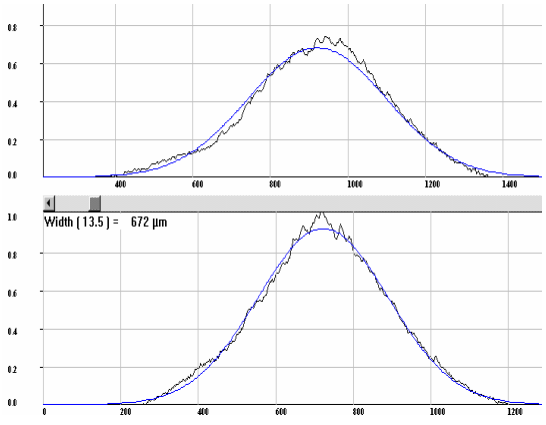

19 A

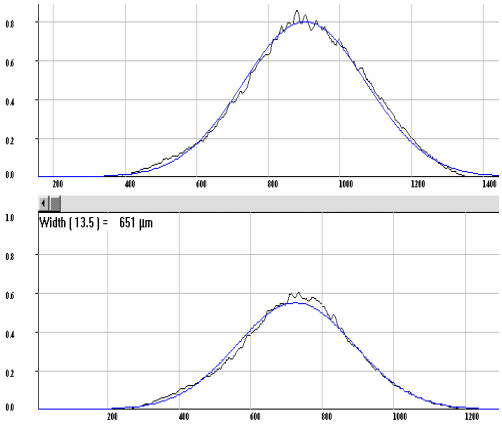

21A

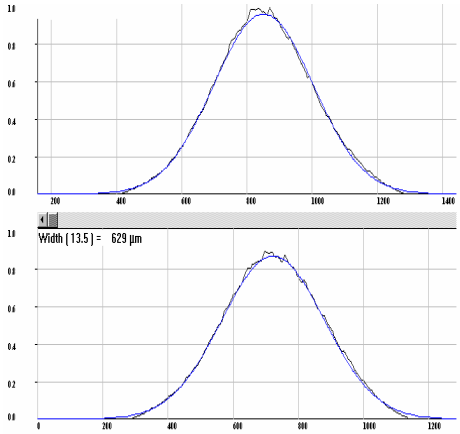

26 A

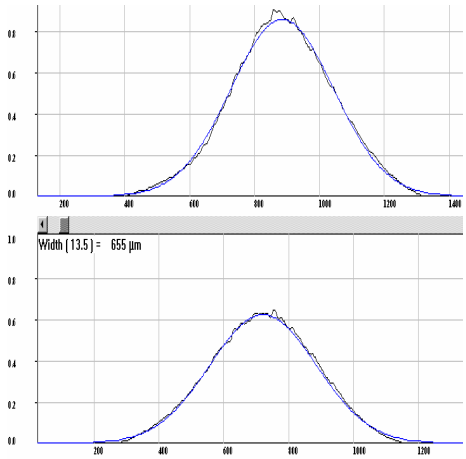

23 A

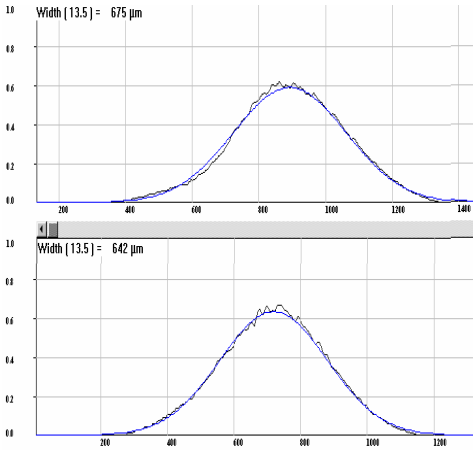

27 A

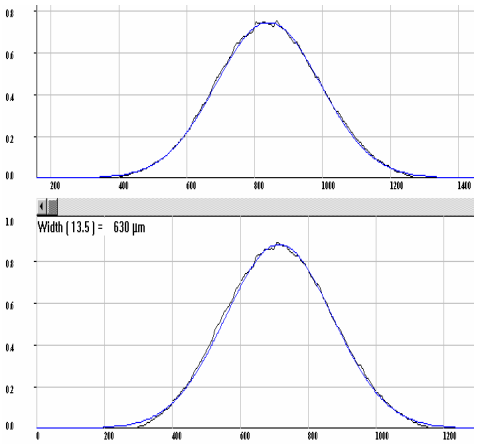

25 A

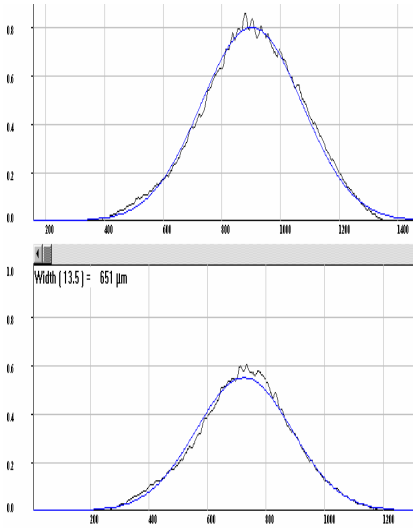

28 A

Fig. 11. Gaussian intensity profiles in vertical and horizontal directions of the beam at arc lamp currents in the range 19-30 A (blue dotted line indicates the theoretical Gaussian fit).

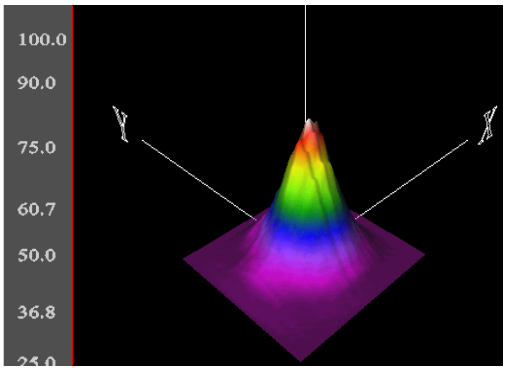

19 A

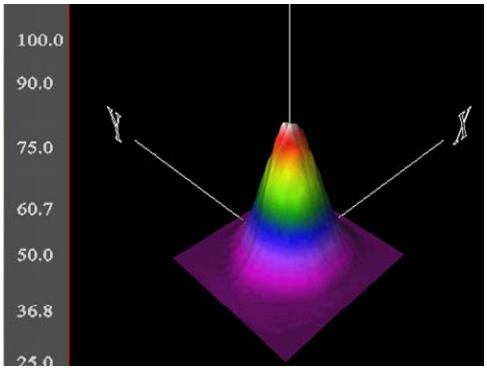

21A

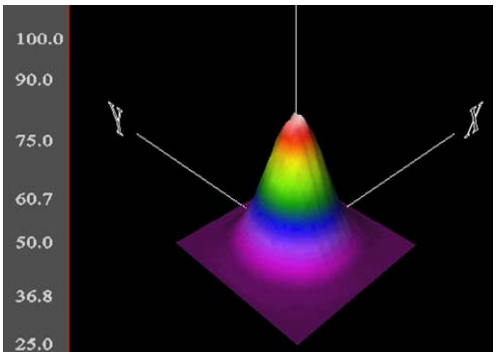

23 A

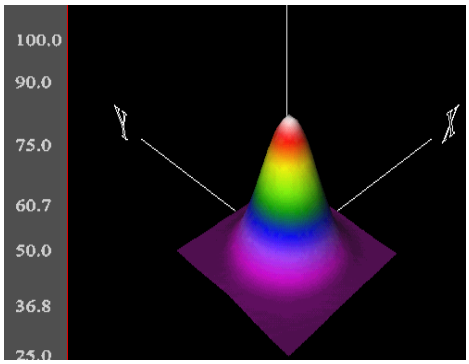

25A

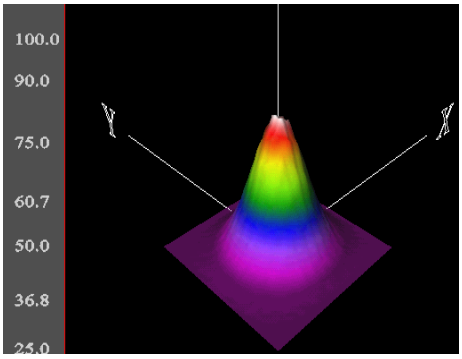

26 A

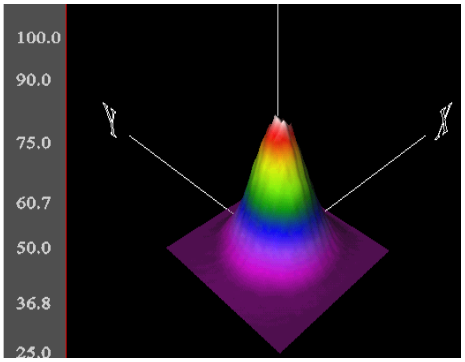

27A

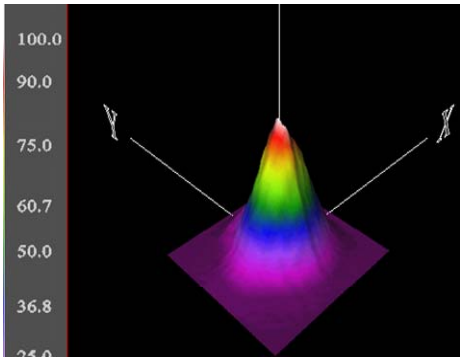

28A

Fig. 12. Three Dimensional intensity Profile of the beam at arc lamp currents in the range 19-28A.

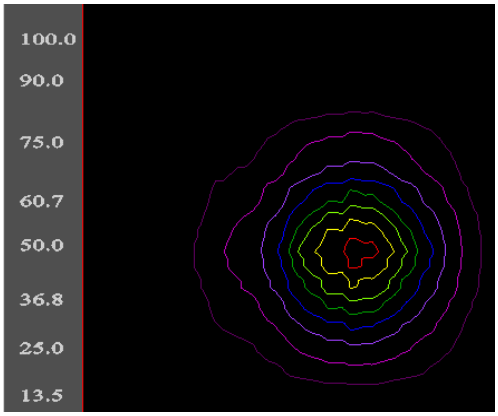

19 A

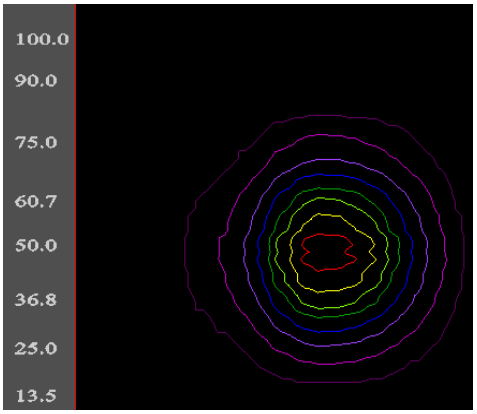

21A

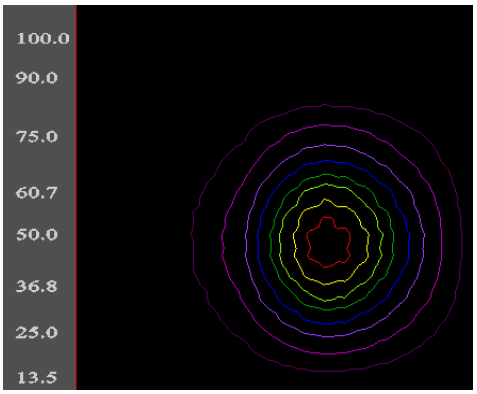

23 A

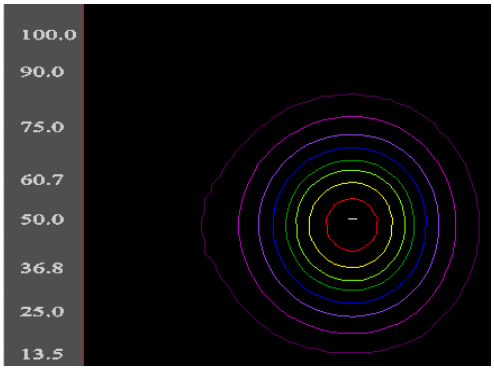

25A

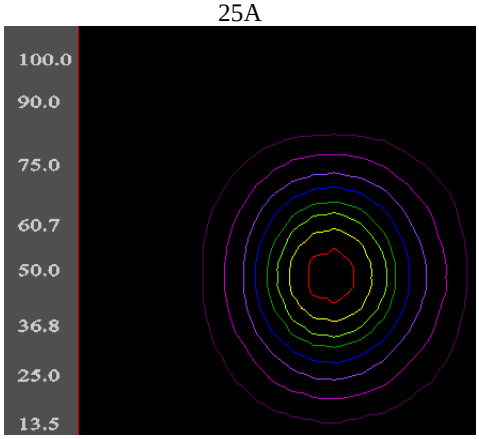

26 A

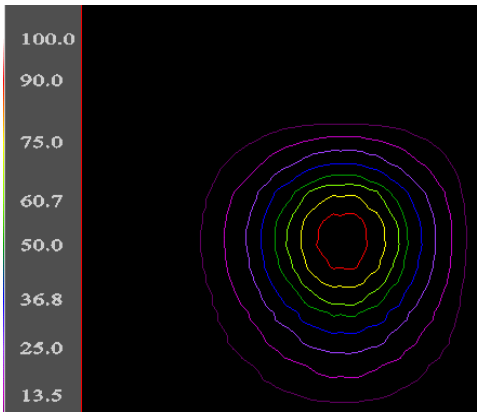

27A

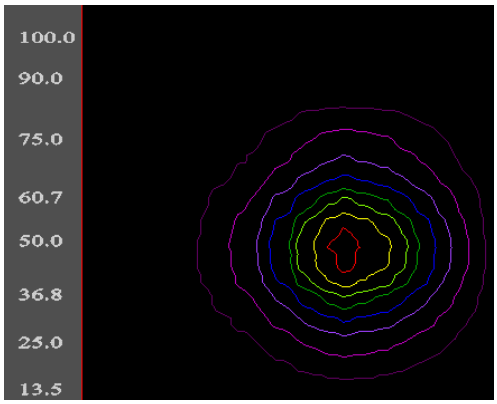

28A

Fig. 13. Three Dimensional intensity Profile of the beam at arc lamp currents in the range 19-30A.

From Figs. 11,12 and 13 it is observed that the laser beam possesses the perfect Gaussian nature and circular beam symmetry when the lamp current is 25A which nearly corresponds to an input pump power of 4200 W .In Section 3.3.1. The value of P_{in}* is obtained as 4055 W for 0.7 at.% doped Nd:YAG crystal. Thus it is once again confirmed that when Pin approaches the value Pin*, beam quality improves where as for values of Pin lower and higher than Pin*, the beam quality deteriorates.

4. Conclusions

It is observed that the beam diameter is minimum for a particular pump power P_{in}* and its value varies with different Nd doping concentration. The input power P_{in}* for which the beam diameter is minimum is calculated for different doping concentrations. The input power P_{in}* for the three Nd doping concentrations are in the order

$$P_{in-0.7}^{*} > P_{in-0.8}^{*} > P_{in-0.65}^{*}$$

The minimum beam diameter w* for these concentrations are in the order

$$w^*_{0.65} < w^*_{0.7} < w^*_{0.8}$$

It is seen that the ellipticity of the beam for 0.7 at.% Nd concentration remains almost unity throughout the complete range of input power. In Table 3.1, it is seen that for the Nd doping concentration of 0.8 at.%, the value of ellipticity first increases from a value of 0.93 to a value near to unity at around P_{in}* (3808.04 W) and then decreases with increase of P_{in} to a value lower than unity. For $P_{in}>P_{in}$* and $P_{in}<P_{in}$* the cross section of the beam is horizontal ellipse where as it approaches circular symmetry at around P_{in}*. For Nd doping concentration of 0.65 at.%, as the input pump power increases, the value of ellipticity also increases from a value less than unity (Fig. 3.4).Hence the cross section of the beam is horizontal ellipse when $P_{in}<P_{in}$*,circular around P_{in}* (3648.82 W) and vertical ellipse when $P_{in}>P_{in}$*. As the 0.7 at.% doped laser crystal exhibits comparatively broad operating range of input pump power over which the output laser beam possess good circular symmetry, it is preferred to others for efficient processing of diamond crystals. Beam diameter $\left(\frac{1}{e^2}\right)$ in horizontal direction is found to be increasing slightly with increase in Pin where as that in vertical direction shows a larger increase. This is an indication that the thermo-optic coefficient values of crystal along these directions are different resulting in different thermal lens focal lengths and beam propagation factors in the respective directions. In the Q-switched operation this is not seen .When the output power is in the range 8-12 Watt, the ellipticity is almost near to unity. Below 8 W, it is found to be less than unity which indicates that the beam is horizontal ellipse. At output power levels greater than 12 W, the ellipticity is much above unity which is showing that the beam cross section is vertical ellipse. This may be due to thermally induced birefringence inside the laser crystal. The variation from horizontal to vertical ellipse with change in average power agrees with the above facts. This measurement is very much helpful to decide a suitable power range within which we can operate the laser can be operated to get nearly perfect circularly symmetric beam for microfabrication of diamond materials to make MOEMS. With increase in average output power of the laser, the full angle divergence decreases first, reaches a minimum value and then increases in both horizontal and vertical directions. In the case of full angle divergence in both directions, it remains almost the same in this range. It can be assumed that the thermo-optic behavior of the laser crystal in this range is uniform in both directions. From the laser beam profiles it is observed that at lower pump powers for which $P_{in} < P_{in}$* and for higher pump powers $P_{in} > P_{in}$*, the beam profile is highly distorted and the deviation from Gaussian intensity distribution is more. The laser beam possess the perfect Gaussian nature and circular beam symmetry when the lamp current is 25A which nearly corresponds to an input pump power of 4200 W. The value of P_{in}* is obtained as 4055 W for 0.7 at.% doped Nd:YAG crystal. Thus it is once again confirmed that when Pin approaches the value Pin*, beam quality improves and this working range is most suitable for using the laser in microfabrication of MOEMS devices. For values of P_{in} lower and higher than P_{in}*, the beam quality becomes worse.

References

[1] M. Cooper, Proceedings of International Diamond Technical symposium, Tel-Aviv, Israel, Oct. (1991).

[2] U. Wittrock, G. Bostanjoglo, S. Dong, B. Eppich, Th. Haase, Quitao Lu N. Muller, O. Holst, SPIE Procedings. 2206 (1998).

[3] S. K. Sudheer, V. P. Mahadevan Pillai, V. U. Nayar. J. Optoelectron. Adv. Mater. **7**, 1047 (2005).

[4] S. K. Sudheer, V. P. Mahadevan Pillai, V. U. Nayar. J. Optoelectron. Adv. Mater. **7,** 1593 (2005).

[5] S. K. Sudheer, V. P. Mahadevan Pillai, V. U. Nayar. Fib. Int. Opt. **25,** 59 (2006).

[6] S. K. Sudheer, V. P. Mahadevan Pillai, V. U. Nayar. Laser Phy. Lett.**3,** 244 (2006).

[7] S. K .Sudheer, V. P .Mahadevan Pillai, V. U. Nayar, "High Repetition Rate Multi-wavelength Polarized Solid State Laser Source for Long Range LIDAR Applications", Proc. of SPIE Vol. **6409**, 64091I, (2006) · doi: 10.1117/12.697759.

[8] T. Dascalu, N. Pavel, M. Poterasu, Optical Resonators-Science and Engineering, Kluwer (1998) Academic Publishers, Dordrecht, Netherlands.

[9] Pranab K. Mukhopadhyay, K Ranganathan, Jogy George, S. K. Sharma, T. P. S. Nathan, Pramana, **58**, 657 (2002).

[10] C. P. Wyss, WLiithy, H. P. Weber, V. I. Vlasov, Yu. D. Zavartsev, P. A. Studenikin, A. I. Zagumennyi, I. A. Scherbakov, Appl. Phys. **B68**, 659 (1999).

[11] T. Jenson, V. G. Osfraumer, J. P. Meyn, G. Huber, A. I. Zagumennyi, I. A. Scherbakov, Appl. Phys. **B58**, 373 (1994).

[12] W. Koechner, D. K. Rice, IEEE J. Quant. Electron. QE-**6**, 557 (1970).

[13] K. B. Steinbruegge, T. Henningsen, R. H. Hopkins, R. Mazelsky, N. T. Melamed, E. P. Riedel, G. W. Roland, Appl. Opt. **11**, 999 (1972).

[14] K. B. Steinbruegge, G. D. Baldwin, Appl. Phys. Lett. **25**, 220 (1972).

[15] M. Born, E. Wolf: Principles of Optics (Pergamon, London, 1965).

[16] J. D. Foster, L. M. Osterink: J. Appl. Phys. **41**, 3656

(1970).
[17] W. Koechner, D. K. Rice: IEEE J. QE-**6**, 557 (1970).
[18] A. Stein: CW YAG laser techniques, Rept, AD 743979, US Army Electronics Command, Fort Monmouth, NJ (1972).
[19] F. W. Quelle: Appl. Opt. **5**, 633 (1966).
[20] E. P. Riedel, G. D. Baldwin: J. Appl. Phys. **38**, 2720 (1967).
[21] W. A. Clarkson, D. C. Hanna, 1998, Optical Resonators-Science and Engineering, Kluwer Academic Publishers, Dordrecht, Netherlands.
[22] W. Koechner, Solid-state laser engineering, Springer-Verlag, Berlin (1999).
[23] R. Ifflaender, Solid-state lasers for materials processing, Springer - Verlag, Berlin (2001).
[24] M. T. Bronski, M. S. Machate, Proc. SEM Graduate Students Symposium., SUNY Stony Brook, Long Island, NY (2002).
[25] D. Mudge, M. Ostermeyer, P. J. Veitch, J. Much, B. Middlemiss, D. J. Ottaway, M. W. Hamilton, IEEE Journal of selected topics in quantum electronics, **6**, 643 (2000).

*Corresponding author: sudheersk@vit.ac.in